Dalton Transactions

Accepted Manuscript

ROYAL SOCIETY OF CHEMISTRY

www.rsc.org/dalton

An Experimental and Theoretical Magneto-Structural Study of Polynuclear Ni^{II} Complexes Assembled from a Versatile bis(salicylaldehyde)diamine Polytopic Ligand

Itziar Oyarzabal,[a] José Ruiz,[b] Antonio J. Mota,[b] Antonio Rodríguez-Diéguez,[b] José M. Seco,*[,a] Enrique Colacio*[,b]

a) Departamento de Química Aplicada, Facultad de Química, Universidad del País Vasco UPV/EHU, Paseo Manuel Lardizabal, nº 3, 20018, Donostia-San Sebastián, Spain. Email: josemanuel.seco@ehu.es.

b) Departamento de Química Inorgánica, Facultad de Ciencias, Universidad de Granada, Av. Fuentenueva S/N, 18071 Granada (Spain). Email: ecolacio@ugr.es.

Abstract

Six novel Ni^{II} complexes, ranging from mononuclear to tetranuclear, have been prepared from the polytopic symmetrical Mannich base ligand N,N'-dimethyl-N,N'-bis(2-hidroxy-3-formyl-5-bromo-benzyl)ethylenediamine (H_2L) and different anionic coligands: $[Ni(H_2L)(NO_3)(H_2O)]NO_3 \cdot H_2O$ (**1**), $[Ni_2(\mu\text{-}L)(acac)_2(H_2O)] \cdot CH_3CN$ (**2**), $[Ni_2(\mu\text{-}L)(\mu\text{-}OAc)(NCS)]$ (**3**), $[Ni_3(\mu\text{-}L)_2(\mu\text{-}OH_2)_2(H_2O)(CH_3CN)](NO_3)_2 \cdot 4CH_3CN$ (**4**), $[Ni_4(\mu\text{-}L)_2(\mu\text{-}OAc)_2(\mu\text{-}OCH_3)_2] \cdot 6H_2O \cdot 2CH_3OH$ (**5**) and $[Ni_4(\mu\text{-}L)_2(\mu\text{-}OAc)_2(\mu\text{-}N_3)_2] \cdot 2H_2O \cdot CH_3OH$ (**6**). These complexes have been characterized by single crystal X-ray diffraction, magnetic measurements and DFT theoretical calculations. The structural analysis of these complexes reveals that the anionic coligand and reaction conditions play a fundamental role in determining their final structures and magnetic properties. Compound **1** contains a monomeric cationic unit with the nickel ion coordinated in the external O_4 site of the compartmental ligand H_2L, which acts in a neutral zwitterionic form. Complexes **2** and **3** are dinuclear Ni_2 neutral entities, in which the Ni^{II} ions are connected through two μ-phenoxido bridging groups. The $Ni(O)_2Ni$ bridging fragment in **2** is almost planar, whereas in **3** is bent due to the additional presence of a *syn-syn* acetate bridge connecting the Ni^{II} atoms. Complex **4** has a bent trinuclear structure with double μ-phenoxido/μ-water bridges between the central and terminal nickel atoms. Complexes **5** and **6** are Ni_4 complexes with defective dicubane structures, in which triple μ-phenoxido/$\mu_{1,1,1}$-X/*syn-syn* acetate and double μ-phenoxido/$\mu_{1,1,1}$-X mixed bridges

connect central and terminal Ni^{II} atoms, whereas double $\mu_{1,1,1}$-X bridging ligands link the central Ni^{II} ions (X = methoxido and azido groups for **5** and **6**, respectively).

Magnetic susceptibility measurements reveal that complex **2** shows a moderate antiferromagnetic interaction between the Ni^{II} ions through the double di-μ-phenoxido bridge, leading to a S = 0 ground state. Compared to **2**, complex **3** shows a much weaker magnetic exchange interaction due the counter-complementarity effect provoked by the additional presence of the *syn-syn* acetate bridging group, as well as the non-planarity of the bridging fragment. In complex **4**, the double μ-phenoxido/μ-water mixed bridges lead to very weak antiferromagnetic interactions between the central and external Ni^{II} ions. Overall ferromagnetic interactions are found for **3**, **5** and **6**, although in **5** not all the magnetic pathways transmit ferromagnetic interactions. A detailed analysis of the magnetic exchange interactions transmitted through the different pathways as well as DFT calculations on the X-ray structures of compounds **2**-**6** were performed to support the magneto-structural data of these compounds.

Introduction

Polynuclear metal complexes with a diversity of bridging ligands are still attracting considerable research interest due to their relevance in fields such as bioinorganic chemistry[1] and magnetic molecular materials.[2] In this regard, it should be noted that Ni^{II} coordination clusters showing global ferromagnetic coupling are promising candidates to present single-molecule magnet (SMM) behaviour, that is to say systems exhibiting slow relaxation of the magnetization and magnetic hysteresis below the so-called blocking temperature, T_B.[3] This is so because Ni^{II} ions are known to exhibit significant magnetic anisotropy (arising from the second order spin-orbit coupling) and because the ferromagnetic coupling leads to a high spin ground state.[4] These two features, magnetic anisotropy and a high spin ground state, are just the main prerequisites to observe SMM behaviour.[3a] The interest in SMMs arises from their outstanding potential technological applications.[5] It is worth noting that only a few examples of nickel(II) single-molecule magnets have been reported so far.[6]

The ground state and magnetic properties of coordination clusters mainly depend on the specific donor sites and bridging modes of the primary and ancillary ligands, as well as on the spin and preferred stereochemistry of the metal ions. Therefore, a better understanding of the structural, electronic and stereochemical factors governing the

magnetic exchange coupling between metal ions through bridging ligands (magneto-structural correlations), as well of the self-assembly process of the building units that leads to the final architecture, would enable us to design coordination clusters with desired magnetic properties. Although magneto-structural correlations are well established for polynuclear Cu^{II} complexes, however, those for the Ni^{II} counterparts,[7] and specifically for mixed-bridged systems,[8] are still limited. Therefore, new examples of Ni(II) complexes with unusual mixed-bridges between the metal ions, that can contribute to the establishment of magneto-structural correlations, are required.

The self-assembly of polytopic ligands containing phenoxide groups (which are able to bridge two Ni^{II} atoms) and anionic ancillary ligands (which balance charge and are also able to act as bridging ligands) allows for the formation of aggregative coordination clusters with a variety of structural types and magnetic properties.[7b,8,9] In this context, we have recently shown, firstly, that the Mannich base hexadentate N_2O_4 ligand *N*,*N*'-dimethyl-*N*,*N*'-bis(2-hydroxy-3-methoxy-5-methylbenzyl)ethylenediamine (H_2L^1) is able to form a wide diversity of phenoxide-bridged Ni^{II} polynuclear complexes, in which the ligand exhibits a high versatility adopting compartmental and open forms with new coordination modes and, secondly, that the anionic coligand (azide, acetate, chloride and acetylacetonate) plays a crucial role in determining the final architecture of the polynuclear Ni^{II} complexes and, consequently, their ground state and magnetic properties.[10]

In this paper we report an extension of our studies on Ni^{II} polynuclear complexes by using the Mannich base hexadentate N_2O_4 ligand N,N'-dimethyl-N,N'-bis(2-hidroxy-3-formyl-5-bromo-benzyl)ethylenediamine (H_2L, see Scheme 1), which is very similar to H_2L^1 but having aldehyde instead of methoxy groups as source of neutral oxygen donor atoms. The difference in chelate rings adopted by the phenoxide and either aldehyde (six-membered ring) or methoxy (five-membered ring) in H_2L and H_2L^1, respectively, is expected to have a significant influence in the adoption of the final structure of the coordination cluster. Specifically, this paper deals with the synthesis, structural characterization, magnetic properties and DFT theoretical calculations of six Ni^{II} complexes containing the H_2L ligand and different anionic coligands (azide, methoxide, acetate and acetylacetonate), which range from mononuclear to tetranuclear. The H_2L ligand acts with different coordination modes (see scheme 1) affording complexes with unusual mixed-bridges between Ni^{II} ions. As expected, the same reactions conditions lead to different compounds for H_2L and H_2L^1 ligands.

Experimental

Materials and Physical Measurements.

All reagents were obtained from commercial sources and used as received. The ligand H_2L (N,N'-dimethyl-N,N'-bis(2-hidroxy-3-formyl-5-bromo-benzyl)ethylenediamine) was prepared following a reported procedure.[11] Elemental (C, H, and N) analyses were performed on a Leco CHNS-932 microanalyzer. IR spectra of powdered samples were recorded in the 400-4000 cm^{-1} region on a Nicolet 6700 FTIR spectrophotometer using KBr pellets. Variable-temperature magnetic susceptibility (2-300 K) and magnetization measurements at 2 K and different magnetic fields (0-50 kOe) were carried out with a Quantum Design SQUID MPMS XL5 magnetometer for **2, 3** and **6** and with a PPMS (Physical Property Measurement System) - Quantum Design Model 6000 magnetometer for **4**. For compound **5**, however, temperature-dependent magnetic susceptibility was measured with a Quantum Design SQUID MPMS-7T device in the 5-300 K temperature range and magnetization measurements were carried out at 0-100 kOe range with a CFMS-VSM-14T (CryoFree Magnet System – Vibrating sample magnetometer). Diamagnetic corrections were estimated from the Pascal´s constants. Alternating current magnetic measurements in a 3.5 G ac field were performed on a PPMS - Quantum Design Model 6000.

Computational Details.

All theoretical calculations were carried out at the density functional theory (DFT) level using the hybrid B3LYP exchange-correlation functional,[12] as implemented in the Gaussian 09 program.[13] A quadratic convergence method was employed in the self-consistent-field process.[14] The triple-ζ quality basis set proposed by Ahlrichs and co-workers has been used for all atoms.[15] Calculations were performed on complexes built from experimental geometries as well as on model complexes. The electronic configurations used as starting points were created using Jaguar 7.9 software.[16] The approach used to determine the exchange coupling constants for polynuclear complexes has been described in detail elsewhere.[17]

Crystallographic Refinement and Structure Solution.

Single crystals of suitable dimensions were used for data collection. For compound **1,** diffraction intensities were collected on an Oxford Diffraction Xcalibur diffractometer

with graphite-monochromated Mo Kα radiation (λ = 0.71069 Å) at 100 (2) K. For the other compounds, intensity data were collected on an Agilent Technologies Super-Nova diffractometer, which was equipped either with monochromated Mo Kα radiation (λ = 0.71069 Å) and Eos CCD detector for **2**, **4** and **6** or monochromated Cu Kα radiation (λ = 1.54180-4 Å) and Atlas CCD detector for compounds **3** and **5**.

In all cases, data frames were processed (unit cell determinations, intensity data integrations, routine corrections for Lorentz and polarization effects and analytical absorption corrections) using the CrysAlis Pro software package.[18] The structures were solved by direct methods and refined by full-matrix least-squares with SHELXL-97.[19] Attempts to solve disorder problems with one acetonitrile crystallization molecule failed in compound **4**, whereas the identification of crystallization solvent molecules in **5** (2 methanol molecules and 6 water molecules) and **6** (2 water molecules and one methanol molecule) was not possible. Instead, a new set of F^2 (*hkl*) values without the contribution from solvent molecules was obtained by the SQUEEZE procedure implemented in PLATON-94.[20]

Final $R(F)$, $wR(F^2)$ and goodness of fit agreement factors, details of the data collection and analysis can be found in Table S1. Selected bond lengths and angles are given in Table S2. CCDC reference numbers for the structures of **1**-**6** are 1043870-1043875.

Syntheses of Complexes.

$[Ni(H_2L)(NO_3)(H_2O)]NO_3 \cdot H_2O$ (**1**)

To a solution of $Ni(NO_3)_2 \cdot 6H_2O$ (0.036 g, 0.125 mmol) in MeOH (5 mL), 0.064 g of H_2L (0.125 mmol) were added. The mixture was stirred for 5 minutes until solution and then was left undisturbed at room temperature. X-ray-quality green crystals were formed from the solution after several days, which were collected by filtration, washed with MeOH and dried in vacuum. Yield: 0.048 g, 52%. Anal. Calcd for $C_{20}H_{26}N_4O_{12}Br_2Ni$. C, 32.77; H, 3,58; N, 7,64. Found: C, 32,88; H, 3,60; N, 7,58.

$[Ni_2(\mu\text{-}L)(acac)_2(H_2O)] \cdot CH_3CN$ (**2**),

To a suspension of $Ni(acac)_2$ (0.064 g, 0.25 mmol) in CH_3CN (5 mL), 0.064 g of H_2L (0.125 mmol) and drops of water were added. The mixture was stirred for 15 minutes and then kept undisturbed until the thin solid was decanted. The resulting

solution was separated and kept at room temperature for several days, affording few X-ray-quality crystals. Yield: 0.009 g, 8%. Anal. Calcd for $C_{32}H_{39}N_3O_9Br_2Ni_2$: C, 43.34; H, 4.43; N, 4.74. Found: C, 43.78; H, 4.55; N, 4.88. Selected FT-IR data (cm^{-1}): ν(acac) 1596vs.

$[Ni_2(\mu\text{-}L)(\mu\text{-}OAc)(NCS)]$ (**3**)

To a solution of $Ni(CH_3COO)_2{\cdot}4H_2O$ (0.062 g, 0.25 mmol) in MeOH (10 mL) were added H_2L (0.064 g, 0.125 mmol) and KSCN (0.122 g, 1.25 mmol). The mixture was stirred for 30 minutes, filtered and the filtrate was kept undisturbed at room temperature. After two days, green crystals of **3** were obtained, which were filtered off, washed with MeOH and dried in vacuum Yield: 0.046 g, 49%. Anal. Calcd for $C_{23}H_{23}N_3O_6SBr_2Ni_2$: C, 37.00; H, 3.11; N, 5.63. Found: C, 37.07; H, 3.15; N, 5.55. Selected FT-IR data (cm^{-1}): ν(thiocyanate) 2105vs, ν_{as}(acetate) 1573vs.

$[Ni_3(\mu\text{-}L)_2(\mu\text{-}OH_2)_2(H_2O)(CH_3CN)](NO_3)_2{\cdot}4CH_3CN$ (**4**)

H_2L (0.064 g, 0.125 mmol), drops of water and Et_3N (0.025 g, 0.25 mmol) were successively added to a solution of $Ni(NO_3)_2{\cdot}6H_2O$ (0.055 g, 0.188 mmol) in CH_3CN (10 mL). The mixture was stirred during 30 minutes and then was filtered to eliminate any amount of insoluble material. The filtrate was allowed to stand at room temperature for a day, whereupon green X-ray quality crystals of **4** were formed. Yield: 0.070 g, 71%. Anal. Calcd for $C_{50}H_{61}N_{11}O_{17}Br_4Ni_3$: C, 37.92; H, 3.88; N, 9.73. Found: C, 37.72; H, 3.94; N, 9.59.

$[Ni_4(\mu\text{-}L)_2(\mu\text{-}OAc)_2(\mu\text{-}OCH_3)_2]{\cdot}6H_2O{\cdot}2CH_3OH$ (**5**)

To a solution of $Ni(OAc)_2{\cdot}4H_2O$ (0.062 g, 0.25 mmol) in MeOH (5 mL) the ligand H_2L (0.064 g, 0.125 mmol) was added and the mixture was stirred for 30 minutes, filtered, and the filtrate left undisturbed at room temperature. After several days, X-ray-quality green crystals were formed, which were collected by filtration, washed with MeOH and dried in vacuum. Yield: 0.062 g, 62%. Anal. Calcd for $C_{48}H_{72}N_4O_{22}Br_4Ni_4$: C, 35.78; H, 4.50; N, 3.48. Found: C, 35.86; H, 4.60; N, 3.56. Selected FT-IR data (cm^{-1}): ν_{as}(acetate) 1567vs.

$[Ni_4(\mu\text{-}L)_2(\mu\text{-}OAc)_2(\mu\text{-}N_3)_2]{\cdot}2H_2O{\cdot}CH_3OH$ (**6**)

This compound was prepared following the same procedure than for **3**, except that NaN_3 (0.08 g, 0.125 mmol) was added instead of KSCN. Yield: 0.052 g, 54%. Anal.

Calcd for $C_{45}H_{54}N_{10}O_{15}Br_4Ni_4$: C, 35.34; H, 3.56; N, 9.16. Found: C, 35.42; H, 3.63; N, 9.05. Selected FT-IR data (cm^{-1}): ν(azide) 2080vs, ν_{as}(acetate) 1560vs.

Results and discussion

The hexadentate N_2O_4 ligand N,N'-dimethyl-N,N'-bis(2-hidroxy-3-formyl-5-bromo-benzyl)ethylenediamine (H_2L) has been prepared in moderate yield via standard Mannich reaction between 2-formyl-4-bromophenol, N,N'-dimethylethylenediamine and formaldehyde following a literature procedure.[11] It should be noted that the coordination chemistry of the H_2L ligand remains almost unexplored and, to the best of our knowledge, only two trinuclear Zn^{II}-Ln^{III}-Zn^{III} complexes (Ln^{III} = Dy, Er) were previously reported, where the deprotonated L^{2-} ligand acts in a compartmental mode with the oxygen atoms of the aldehyde groups coordinated to the Ln^{3+} ion (see scheme 1, coordination mode c).[21]

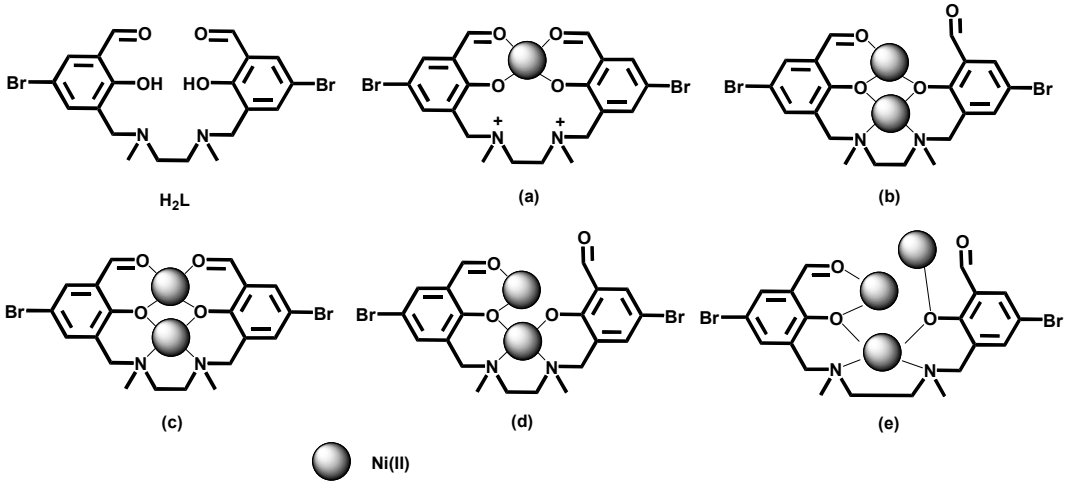

Scheme 1. Structure of H_2L and its coordination modes

The reaction of the H_2L ligand with $Ni(NO_3)_2 \cdot 6H_2O$ in a 1:1 molar ratio and using methanol as solvent afforded the mononuclear cationic complex **1** (see Scheme 2), in which the protons migrate from the phenolic oxygen atoms to the nitrogen atoms and, as a result, the ligand shows a zwitteronic coordination mode *a* (see scheme 1). The reaction of $Ni(acac)_2$ with H_2L in a mixture acetonitrile/water, using a H_2L/Ni^{II} 1:2 molar ratio led to the dinuclear complex **2**, where the deprotonated ligand exhibits the coordination mode *b* (see schemes 1 and 2). The basic character of the acetylacetonate anion allows for the

deprotonation of the ligand. The addition of triethylamine and drops of water to a solution of the ligand and $Ni(NO_3)_2 \cdot 6H_2O$ (H_2L/Ni^{II} 1:1.5 molar ratio) in acetonitrile allowed for the preparation of green crystals of the bent trinuclear complex **4**, in which the fully deprotonated ligand exhibits the coordination mode *d*.

The reaction between $Ni(OAc)_2 \cdot 4H_2O$ and H_2L in methanol and using a H_2L /Ni^{II} 1:2 leads to the formation of the tetranuclear face-sharing defective dicubane complex **5**. In the formation process, two open dinuclear $[Ni_2L_2(\mu\text{-OAc})]^+$ building units are assembled by methoxido anions that occupy two vertices of the common face of the final defective dicubane structure. The ligand exhibits the coordination mode *e* and its deprotonation is provoked by the basic acetate anion. Although methanol is a weaker acid than acetic acid and therefore the formation of methoxide anion from a solution of acetate in methanol is not favoured, however, the very small amount of methoxide anion in the equilibrium may be enough to connect the $[Ni_2L_2(\mu\text{-OAc})]^+$ units shifting the reaction to the formation of complex **5**. The same reaction as for **5**, but using NaN_3 in a 1:2:1 $H_2L/Ni^{II}/NaN_3$ molar ratio afforded the tetranuclear face-sharing defective dicubane complex **6**, in which the azide anions occupy the same positions as the methoxide anions in the isostructural complex **5**. Using the same reaction conditions as for the formation of **5** and an excess of KSCN (1:5 Ni/KSCN ratio), the dinuclear compound **3** was obtained, in which the ligand is fully deprotonated and exhibits a coordination mode *c*.

All these results clearly show the important role of the anionic coligand (X), solvent and ratio of reactants in determining the final architecture of the $L/Ni^{II}/X$ system. A summary of the different complexes obtained from the $H_2L/Ni/X$ reacting systems is given in Scheme 2.

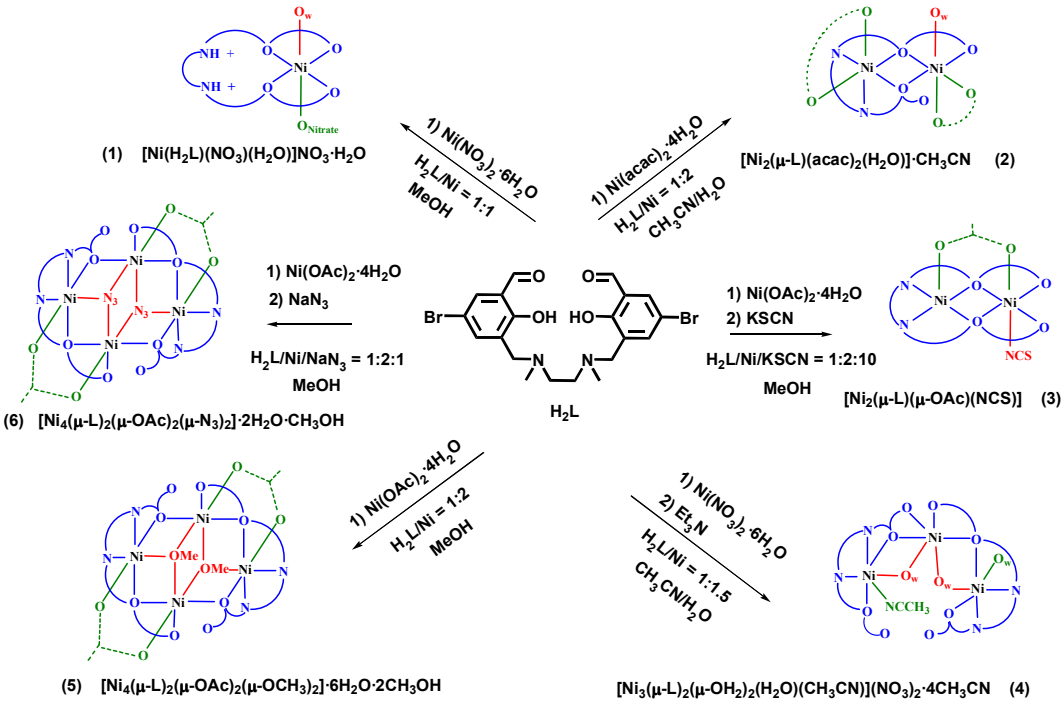

Scheme 2. Reactivity of the H_2L ligand and complexes prepared in this work.

Description of the structures

The crystal structure of **1** is shown in Figure 1 and consists of mononuclear $[Ni(H_2L)(NO_3)(H_2O)]^+$ cationic units, nitrate anions and one crystallization water molecule, all involved in hydrogen bond interactions. Selected bond lengths for **1** are given in Table S2 (ESI). Within the mononuclear $[Ni(H_2L)(NO_3)(H_2O)]^+$ unit, the ligand is coordinated to the Ni^{II} ion in a O4 neutral zwitterionic form through the two deprotonated phenolic oxygen atoms and the two aldehyde oxygen atoms, therefore acting in a 1κ-O_{1A}, 1κ-O_{2A}, 1κ-O_{3A}, 1κ-O_{4A}-tetradentate coordination mode (O_{2A} and O_{3A} represent the phenolic oxygen atoms). The zwitterionic is formed by proton migration from the phenolic oxygen atoms to the nitrogen atoms. Analogous processes have been observed for other complexes containing bis(phenol)diamine Mannich and Schiff base ligands.[22] The Ni^{II} ion exhibits a NiO_6 distorted octahedral coordination environment, in which the O4 donor atoms of the ligand H_2L are located at the equatorial positions, whereas the coordinated water molecule (O1W) and the coordinated nitrate group (O1C) occupy the axial positions.

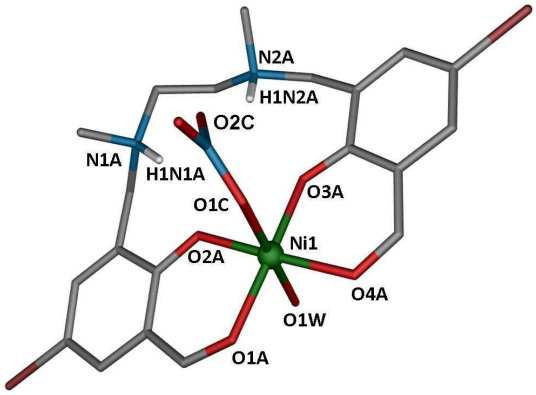

Figure 1. Perspective view of the cationic unit in **1**. Nickel, oxygen, nitrogen, carbon and bromine atoms are in light green, red, light blue, grey and brown, respectively. Nitrate counteranion, hydrogen atoms (except H1N1A and H1N2A, in white) and solvent molecules are omitted for the sake of clarity.

The Ni-O distances are found in the 1.965(2)-2.123(2) Å ranges, those involving the phenoxide groups being significantly shorter than those involving the aldehyde oxygen atoms, as expected. The variation in angles between *trans* donor atoms at the metal centre is very small (1º), whereas the variation in cisoid angles spans a wide range 87.17(9)-92.84(9)º. The aromatic rings of the ligand are practically planar (dihedral angle 3.83º).

The protonated nitrogen atoms N1A and N2A of the zwitterions are involved in moderate intramolecular hydrogen bond interactions with the oxygen atom O2C of the coordinated nitrate group and the nearest phenolic oxygen atoms (O2A and O3A) of the ligand, with O···N distances in the 2.648(4)-2.895(4) Å range (Supporting Information, Figure S1). In addition, the coordinated and non-coordinated water and the nitrate counteranion are involved in an intricate hydrogen bond network with O···O distances in the range of 2.710(4)- 2.764(4) Å.

Compound **2** is formed by a neutral dinuclear [Ni(acac)(μ-L)Ni(acac)(H_2O)] (acac = acetylacetonate) unit and one crystallization acetonitrile molecule. A perspective view of the structure is given in Figure 2, whereas selected bond lengths and angles are given in Table S2. In the dinuclear unit, the ligand acts in a 2κ–O_{1A}, 1κ-O_{2A}:2κ-O_{2A}, 1κ^2-N,N', 1κ-O_{3A}:2κ-O_{3A} pentadentate bridging mode (O_{2A} and O_{3A} represent the phenolic oxygen atoms), which is represented as coordination mode *b* in scheme 1.

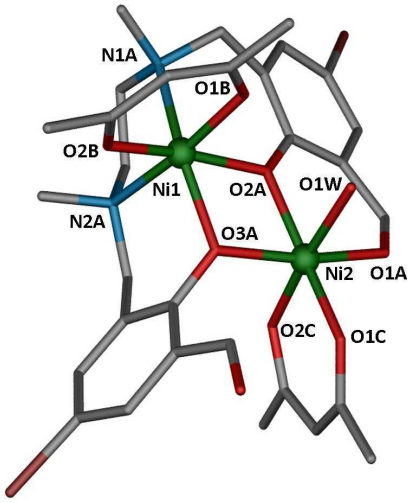

Figure 2. Perspective view of the molecular structure of **2**. Nickel, oxygen, nitrogen, carbon and bromine atoms are in green, red, blue, grey and brown, respectively. Hydrogen atoms and solvent molecules are omitted for the sake of clarity.

Within the [Ni(acac)(μ-L)Ni(acac)(H_2O)] dinuclear unit there exist two independent nickel atoms, labelled Ni1 and Ni2, which are bridged by two μ_2-phenoxido oxygen atoms (O2A and O3A). Both Ni^{II} ions exhibit distorted octahedral coordination environments. The Ni1 atom displays a NiN_2O_4 coordination sphere which is made by two nitrogen atoms and two phenoxido-bridging oxygen atoms of the deprotonated ligand (L^{2-}) and two oxygen atoms of the coordinated acac chelate coligand. In the case of Ni2, the NiO_6 coordination sphere is formed by the oxygen atoms that belong to the two phenoxido-bridges and one aldehyde group (O1A) of the ligand, the second acac chelate coligand and a coordinated molecule of water. The Ni-O distances are in the ranges 2.011(3)-2.125(2) Å and 1.980(2)-2.091(2) Å for Ni1 and Ni2, respectively, whereas the Ni···Ni distance of 3.203(1) Å is comparable to those found in other similar dinuclear nickel(II) complexes having a diphenoxido bridge.[23]

Due to a non planar configuration of the ligand, the dihedral angle between aromatic rings is 79.94º. Each bridging phenoxido oxygen atom is asymmetrically bounded, with one Ni–O bond slightly longer [Ni1–O2A 2.125(2) Å; Ni(1)–O3A 2.060(2) Å] than the other [Ni2–O2A 2.032(2) Å, Ni2–O3A 2.058(2) Å]. The two phenoxido bridging angles, Ni1–O2A–Ni2 and Ni1–O3A–Ni2 are 100.79(7)º and 102.16(8)º, respectively, and the Ni_2O_2 group is practically planar with a dihedral angle between the two O-Ni-O planes (hinge angle, β) of 8.86°. Finally, the mean value of the

out-of-plane displacements of the O-C bond belonging to the phenoxido bridging group from the NiONi plane are 40.35° and 1.45º for O2A–C3A and O3A-C15A bonds, respectively.

The dinuclear Ni_2 units are held together in pairs by a couple of symmetrically related hydrogen bonds involving the non-coordinated carbonyl oxygen atom (O4) of one molecule and the oxygen atom of the coordinated water (O1W) of the adjacent molecule, with a O···O distance of 2.778(3) Å.

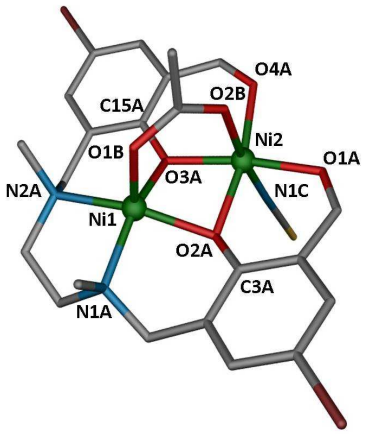

Figure 3. Perspective view of the molecular structure of **3**. Nickel, oxygen, nitrogen, carbon and bromine atoms are in light green, red, light blue, grey and brown, respectively. Hydrogen atoms are omitted for the sake of clarity.

The structure of **3** is made of neutral dinuclear [Ni(μ-L)(μ-OAc)Ni(NCS)] units, in which the Ni^{2+} ions are bridged by two phenoxido groups of the deprotonated (L^{2-}) ligand (adopting the compartmental coordination mode *c* in Scheme 1) and one syn–syn acetate anion. The inner site of the ligand is occupied by a Ni(II) ion that exhibits a NiN_2O_3 square pyramidal coordination sphere. In this description, the two nitrogen atoms and the two phenoxide-bridging oxygen atoms of the ligand are located at the basal positions, whereas the apical position is occupied by an oxygen atom of the acetate bridge. The outer Ni^{2+} ion exhibits a slightly distorted NiO_5N octahedral coordination sphere, which is made by the two phenoxide bridging oxygen atoms, the two aldehyde oxygen atoms, one oxygen atom of the acetate bridging group and the nitrogen atom that belongs to the SCN^- group. The acetate oxygen atom and the nitrogen atom are located in *trans* positions and, consequently, the oxygen atoms of the ligand are located in the equatorial plane of the slightly distorted octahedron. The Ni··O and the Ni··N distances are around 2 Å, whereas the Ni··Ni distance is 2.954(1) Å.

The bridging acetate group forces the structure to be folded with a hinge angle (β) for the Ni(μ-O_2)Ni bridging fragment of 33.60°. As a consequence of the structure folding, the Ni–O–Ni bridging angles (θ) and the intra-dinuclear Ni···Ni distance decrease with respect to those observed in **2** to reach values of 94.1(1)°, 95.4(1)° and 2.955(1) Å, respectively. The values of the out-of-plane displacements of the O-C bonds belonging to the phenoxido bridging groups from the Ni1(O2A)Ni2 and Ni1(O3A)Ni2 planes are 42.75° and 31.35º, respectively.

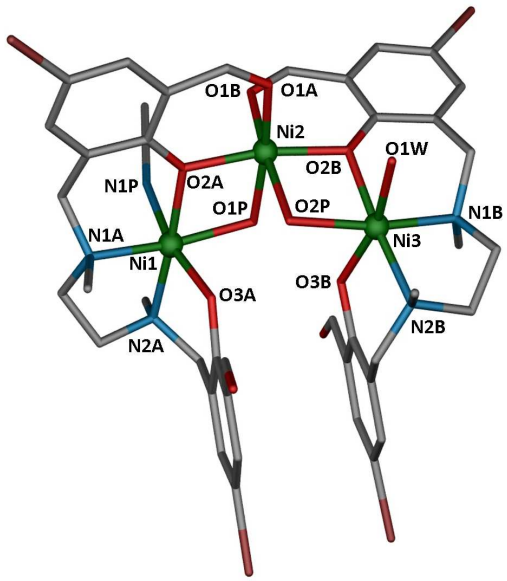

Figure 4. Perspective view of the cationic unit of **4**. Nickel, oxygen, nitrogen, carbon and bromine atoms are in light green, red, light blue, grey and brown, respectively. Hydrogen atoms, nitrate counteranions and solvent molecules are omitted for the sake of clarity.

Compound **4** is made of bent trinuclear asymmetric cationic entities of formula $[Ni_3(\mu\text{-}L)_2(\mu\text{-}OH_2)_2(H_2O)(CH_3CN)]^{2+}$, two nitrate anions and four crystallization acetonitrile molecules (Figure 4). All the Ni^{II} ions of the trinuclear unit are crystallographically independent. The central Ni2 ion is connected to the outer Ni1 and Ni3 ions through two double phenoxido/water bridging groups. The μ-phenoxido groups belong to two different fully deprotonated L^{2-} ligands (labelled A and B), which adopt a 2κ-O_1, 2κ–O_2:nκ–O_2, nκ^2-N, N', nκ-O_3 (n is 1 or 3) pentadentate coordination mode, with bridging and monocoordinated phenoxido groups and uncoordinated and monocoordinated aldehyde groups (coordination mode *d* in scheme1).

The central Ni2 atom exhibits a distorted octahedral NiO_6 coordination sphere, which is formed by the two water bridging molecules in *cis* positions, the two phenoxido-

bridging oxygen atoms in *trans* positions and two aldehyde oxygen atoms (O1A and O1B) belonging to two different L^{2-} ligands in a *cis* arrangement. The outer Ni1 ion presents a distorted octahedral NiN_3O_3 coordination environment, which is made by the two amine nitrogen atoms, one monocoordinated phenoxido oxygen atom (O3A), the phenoxido-bridging oxygen atom (O2A) of the same deprotonated L^{2-} ligand, the nitrogen atom of the coordinated acetonitrile molecule (N1P) and the oxygen atom of the water bridging group (O1P).The three oxygen atoms and, consequently, the three nitrogen atoms are in *fac* dispositions. In the case of outer Ni3, the NiN_2O_4 coordination environment is similar to that of Ni1 but the acetonitrile molecule is replaced by a water molecule.

The Ni-O distances are in the 1.983(3)-2.137(3) Å range (selected bond length and angles are given in Table S2). The values of the out-of-plane displacements of the O-C bonds belonging to the phenoxido bridging groups from the Ni1(O2A)Ni2 and Ni3(O2B)Ni2 planes are 5.3° and 10.05°, respectively.

It should be noted that each water bridge molecule forms a bifurcated hydrogen bond (Supporting Information Figure S2) involving the monocoordinated phenoxido groups with a O···O donor acceptor mean distance of 2.582 Å and one of the nitrate counteranions with a O···O donor acceptor mean distance of 2.666 Å. The former hydrogen bonds are the main responsible for the bent conformation of the Ni_3 molecules. The nitrate anion is involved in an additional hydrogen bond with the water molecule coordinated to Ni3 belonging to a neighbouring trinuclear unit (O···O donor acceptor distance of 2.723 Å), giving rise to a chain running along the *b* axis (see Figure S3). Neighbouring Ni···Ni intramolecular distances are 3.136(1) Å and 3.118(1) Å, whereas the shortest Ni···Ni intertrinuclear distance is 8.143(1) Å.

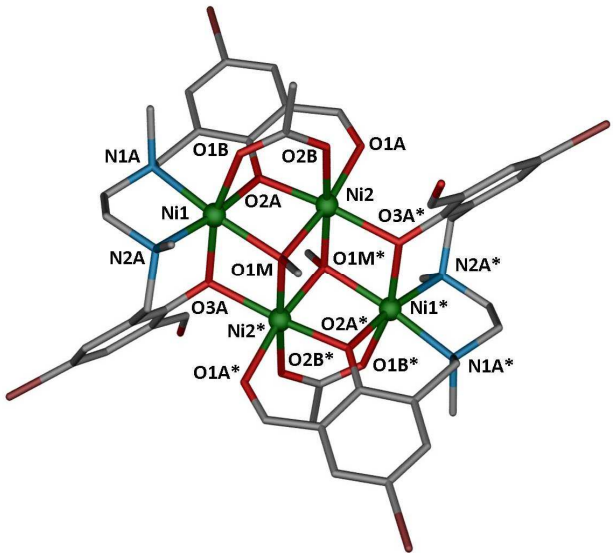

Figure 5. Perspective view of the molecular structure of **5**. Nickel, oxygen, nitrogen, carbon and bromine atoms are in light green, red, light blue, grey and brown, respectively. Hydrogen atoms and solvent molecules are omitted for the sake of clarity.

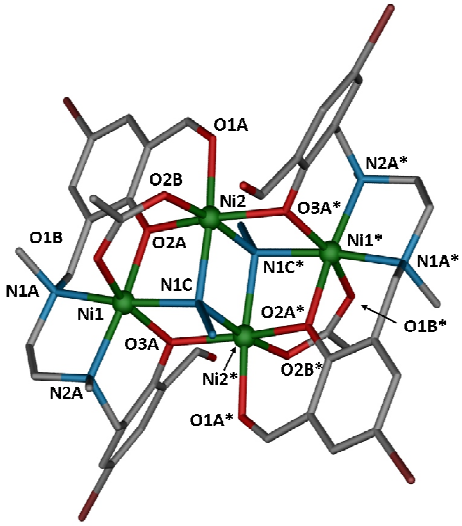

Figure 6. Perspective view of the molecular structure of a Ni4 unit in **6**. Nickel, oxygen, nitrogen, carbon and bromine atoms are in light green, red, light blue, grey and brown, respectively. Hydrogen atoms and solvent molecules are omitted for the sake of clarity.

The crystal structures of the tetranuclear complexes **5** and **6** are shown in Figures 5 and 6, respectively. The structure analysis reveals that both complexes are made of centrosymmetric tetranuclear Ni^{II} units, containing two deprotonated (L^{2-}) ligands, two *syn-syn* acetate bridging groups and two triple $\mu_{1,1,1}$-bridging groups (either methoxido or azide), and solvent crystallyzation molecules (six water and two methanol molecules for **5** and two water and one methanol molecules for **6**). In compound **6** two identical

crystallographic independent Ni_4 units that differ slightly in bond lengths and angles are present. Both compounds exhibit very similar face-sharing defective dicubane-like cores with two missing vertices. The common face of the defective dicubane unit in **5** and **6** is formed by two crystallographically related Ni2 and Ni2* atoms and either the oxygen atom of the $\mu_{1,1,1}$-methoxido bridging groups in the former or the N1 and N1' nitrogen atoms of the $\mu_{1,1,1}$-end-on azide bridging groups in the latter.

In both complexes, the dideprotonated ligand L^{2-} is coordinated to the Ni(II) ions by the two amine nitrogen atoms, the two phenoxido oxygen atoms, which bridge Ni1 and Ni2 atoms and occupy vertices of the dicubane core, and one of the aldehyde oxygen atoms, thus exhibiting a 2κ-O_{1A}, 2κ-O_{2A}:1κ-O_{2A}, 1κ^2-N, N', 1κ-O_{3A}:2κ-O_{3A}, pentadentate coordination mode (mode *e* in Scheme 1). In addition to the phenoxido bridge, the metal centers Ni1 and Ni2 are also bridged by a *syn-syn* acetate group, whereas either $\mu_{1,1,1}$-methoxido or $\mu_{1,1,1}$- azide bridging groups connect two crystallographically equivalent Ni2 atoms between them and with each Ni1 atom. The two couples of centrosymmetrically related nickel atoms exhibit octahedral coordination geometry. In **5**, the Ni1 atoms show NiN_2O_4 coordination environments formed by two nitrogen and two phenoxido-bridging oxygen atoms belonging to the same ligand (L^{2-}), one oxygen atom, O(1B), from the acetate bridging group and one oxygen atom, O(1M), from the $\mu_{1,1,1}$-methoxido group. The Ni2 atoms exhibit NiO_6 coordination spheres, which are formed by the coordination of two phenoxido-bridging oxygen atoms belonging to two different ligands O(2A), O(3A), one oxygen atom from the acetate bridging group (O2B), one aldehyde oxygen atom O(1A) and the two $\mu_{1,1,1}$-methoxido oxygen atoms. The coordination environments around Ni1 and Ni2 atoms in **6** are similar to those observed in **5**, but changing the oxygen atoms of the $\mu_{1,1,1}$-methoxido bridging groups by the nitrogen atoms of the $\mu_{1,1,1}$-azide bridging groups, and therefore exhibit NiN_3O_3 and NiN_2O_4 octahedral coordination polyhedra, respectively.

The Ni atoms in **5** and **6** have a similar environment and follow a similar trend in their bond distances; the largest Ni-O distances corresponding to the phenoxo oxygen atoms O(3A). The Ni-X-Ni (X=O/N) bridging angles span a wide range of values varying between 93.8(1)-103.8(1)° for **5** and 91.1(2)-102.9(2)° for **6**. The Ni2-(μ-O_2)Ni2* and Ni2-(μ-N_2)Ni2* bridging fragments are coplanar, whereas the mean hinge angle for the double μ-phenoxido/$\mu_{1,1,1}$-methoxido or μ-phenoxido/$\mu_{1,1,1}$-azido bridged Ni_2 fragments

is of 6.03° for **5** and 6.90° for **6**. As expected, the additional *syn-syn* acetate bridge in the third bridging fragment increases the mean hinge angle to 19.15° and 19.92° in **5** and **6**, respectively. The Ni1···Ni2 and Ni2··Ni2* mean distances are 3.110 Å and 3.067 Å, respectively, for **5** and 3.149 and 3.172 Å, respectively, for **6**. Bond lengths and angles in the coordination environment of the Ni(II) atoms in **5** and **6** are listed in Table S2.

Magnetic properties

The temperature dependence of the $\chi_M T$ product for complexes **2**-**6** (χ_M being the molar paramagnetic susceptibility of the compound) under a constant magnetic field of 0.1 T in the 2-300 K range are displayed in figures 7-11, respectively.

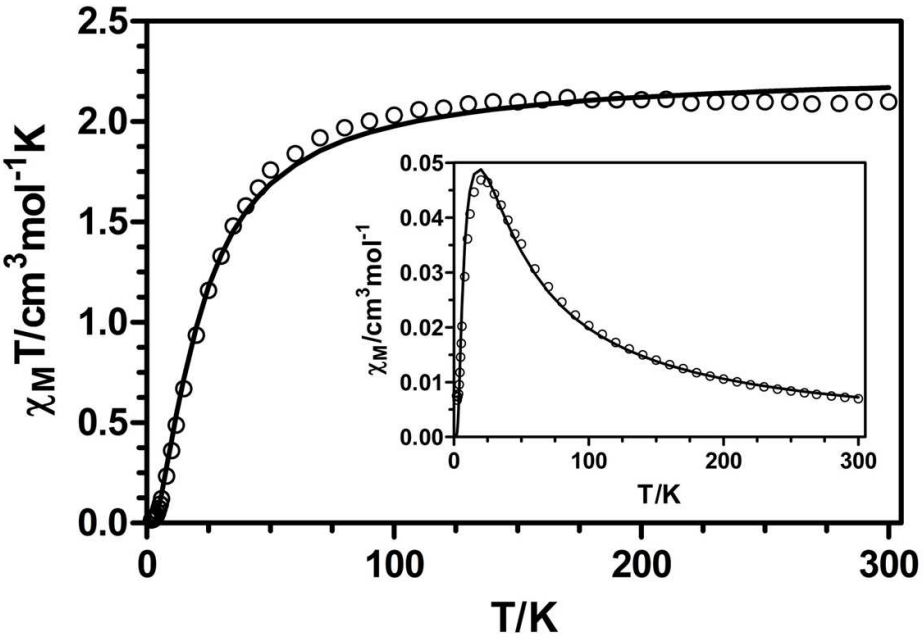

Figure 7. Temperature dependence of the $\chi_M T$ product for **2** in the 2-300 K range. Inset: temperature dependence of the χ_M for **2**. The solid lines are generated from the best fit to the magnetic parameters

At room temperature the $\chi_M T$ value for complex **2** is 2.1 $cm^3 \cdot K \cdot mol^{-1}$, which is in good agreement with the expected value for two non-interacting Ni^{2+} ions (S = 1) with g = 2.0 (2.0 $cm^3 \cdot K \cdot mol^{-1}$). When the temperature is lowered, the $\chi_M T$ product remains almost constant until 100 K, and then drops abruptly to reach a value very close to zero at 2 K. This magnetic behaviour points out the presence of antiferromagnetic exchange interactions within the Ni (II) dinuclear unit. In keeping with this, the thermal variation of the χ_M shows a maximum at 20 K.

The magnetic behaviour of complex **2** has been modelled using the following Hamiltonian:

$$H = -JS_{Ni1}S_{Ni2} + \sum_{i=1}^{2} D_{Ni}S_{Niz}^2 - zJ'\langle S_z \rangle S_z$$

where J is the magnetic exchange pathway through the di-μ-phenoxido double bridge and D_{Ni} is the axial single ion zero field splitting parameter, which is assumed to be the same for both Ni^{2+} ions, and $-zJ'<S_z>S_z$ accounts for the intermolecular interactions by means of the molecular field approximation. Since zJ' and D_{Ni} are strongly correlated and provoke the same result at low temperature, and in view of the fact that influence of D is a very weak effect compared to the intramolecular antiferromagnetic interaction, very difficult to evidence from the magnetic susceptibility data,[9a,24] the magnetic data were analysed by using the isotropic spin Heisenberg Hamiltonian, in which the local anisotropy of the Ni^{II} ions and the intermolecular interactions were not taken into account. The fit of the experimental susceptibility data using the full-matrix diagonalization PHI program[25] afforded the following set of parameters: J = -12.6 cm^{-1} and g = 2.13 with R = 6.5 x 10^{-4} ($R= \Sigma[(\chi_M T)_{exp.} - (\chi_M T)_{calcd.}]^2/\Sigma((\chi_M T)_{exp})^2$). The antiferromagnetic exchange observed in complex **2** leads to a diamagnetic ground state ($S_T = 0$) as confirmed by the isothermal magnetization measurements at 2 K, which show values lower than 0.05 μ_B at high fields (Figure S4, ESI).

On the other hand, complexes **3** and **4** show slightly higher $\chi_M T$ values at room temperature (2.58 $cm^3 \cdot K \cdot mol^{-1}$and 3.83 $cm^3 \cdot K \cdot mol^{-1}$, respectively) than those expected for two and three uncoupled Ni^{2+} (S = 1) ions, respectively, with g = 2.0 (2.0 $cm^3 \cdot K \cdot mol^{-1}$ for **3** and 3.0 $cm^3 \cdot K \cdot mol^{-1}$ for **4**). On lowering temperature, the $\chi_M T$ products for **3** and **4** remain almost constant until 20 K and then drop abruptly reaching values of 1.38 $cm^3 \cdot K \cdot mol^{-1}$ and 2.44 $cm^3 \cdot K \cdot mol^{-1}$ at 2 K, respectively. This behaviour suggests the existence of very weak intramolecular magnetic interactions between the Ni^{II} ions in these complexes (either F or AF) together with intermolecular antiferromagnetic interactions and/or zero field splitting effects promoted by the local anisotropy of the Ni^{II} ions, which are the main responsible for the decrease of $\chi_M T$ at very low temperature.

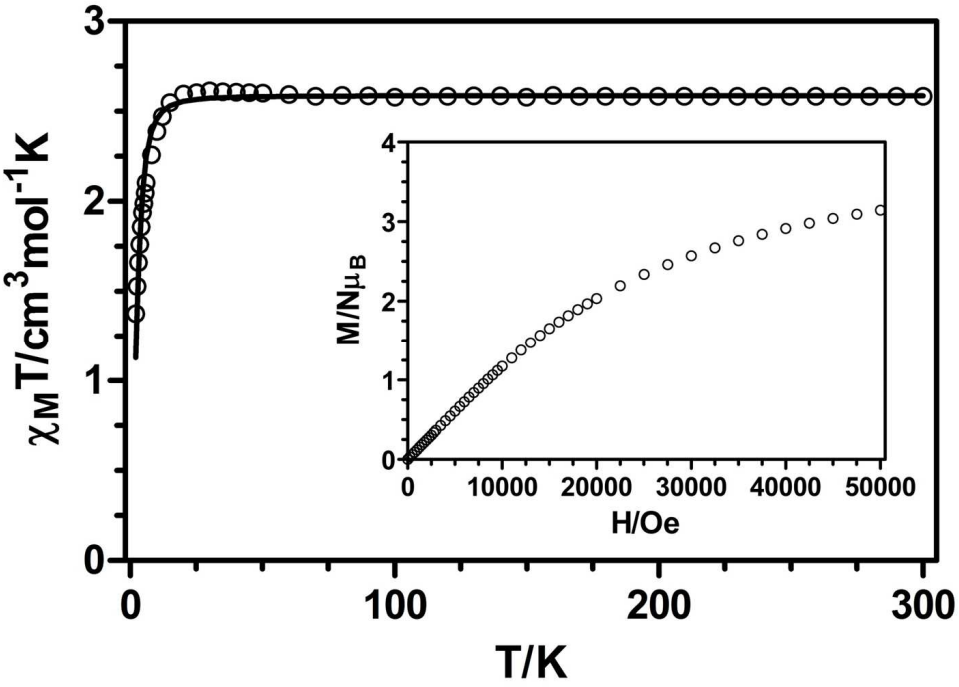

Figure 8. Temperature dependence of the $\chi_M T$ product for **3** in the 2-300 K range. The solid line is generated from the best fit to the magnetic parameters. Inset: field dependence of the magnetization for **3**.

The experimental susceptibility values for **3** and **4** were analyzed with the respective Hamiltonians that takes into account the isotropic interaction between the Ni^{II} centres and their axial single ion zero field splitting parameters. However, different set of parameters with very small positive and negative *J* values and similar R values were obtained from the corresponding fitting procedures. In view of this, we decided to model the experimental susceptibility data for complexes **3** and **4** taking into account only the single ion zero field splitting parameter. The best fit of the experimental data led to the following set of parameters: g = 2.27 and $D = 6.26\ cm^{-1}$ with $R = 6.96 \times 10^{-4}$ for **3** and g = 2.26 and $D = 4.21\ cm^{-1}$ with $R = 3.8 \times 10^{-5}$ for **4**. Negative values of *D* led to worse fits of the susceptibility data. The extracted *D* parameters include the effects of intra- and intermolecular magnetic exchange interactions.

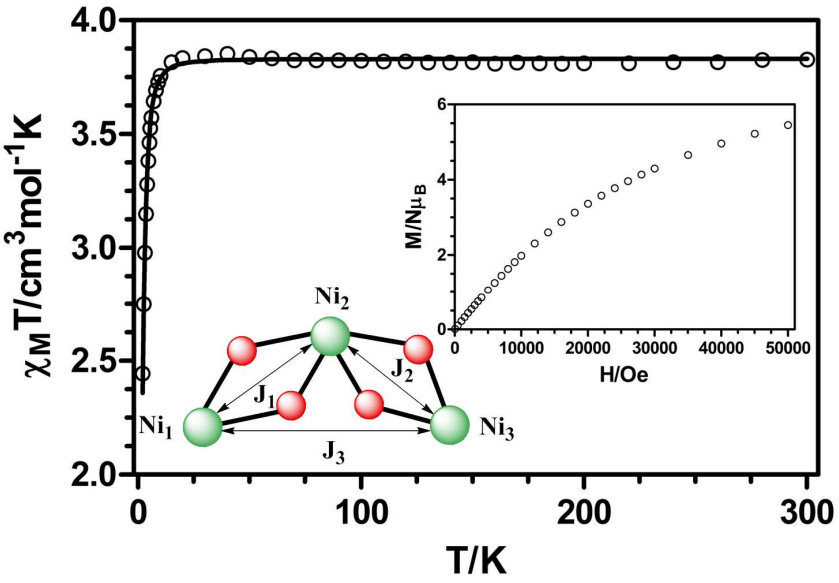

Figure 9. Temperature dependence of the $\chi_M T$ product for **4** in the 2-300 K range. The solid line is generated from the best fit to the magnetic parameters. Inset left: magnetic exchange pathways in compound **4**. Inset right: field dependence of the magnetization for **4**.

The field dependence of the molar magnetization at 2 K for compounds **3** and **4** shows a gradual increase with the applied external field without reaching a complete saturation at 5 T. This behaviour is due to the presence of significant anisotropy and/or low-lying excited states that are partially (thermally and field-induced) populated, which are in agreement with the weak magnetic interactions observed for these complexes.

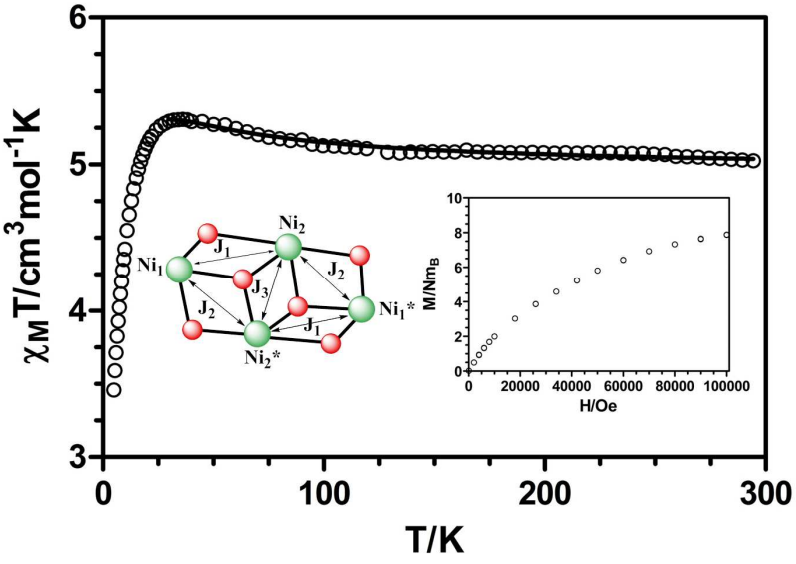

Figure 10. Temperature dependence of the $\chi_M T$ product for **5** in the 5-300 K range. The solid line is generated from the best fit to the magnetic parameters. Inset left: magnetic exchange pathways in compound **5**. Inset right: field dependence of the magnetization for **5**.

To end up, the $\chi_M T$ values at room temperature for the tetranuclear compounds (5.03 $cm^3 \cdot K \cdot mol^{-1}$ for **5** and 5.31 $cm^3 \cdot K \cdot mol^{-1}$ for **6**) are significantly higher than the expected value for four uncoupled Ni^{2+} ions with g = 2.0 (4.0 $cm^3 \cdot K \cdot mol^{-1}$), which is mainly due to the orbital contribution of the Ni^{II} ions. On cooling, the $\chi_M T$ product steadily increases to reach a maximum at 36 K (5.31 $cm^3 \cdot K \cdot mol^{-1}$) and 8.0 K (10.6 $cm^3 \cdot K \cdot mol^{-1}$) for **5** and **6**, respectively. Below these temperatures, $\chi_M T$ decreases quite fast reaching values of 3.46 cm^3 K for **5** at 5 K and 9.81 cm^3 K mol^{-1} for **6** at 2 K. This magnetic behaviour indicates the presence of ferromagnetic exchange interactions between the Ni^{2+} ions together with antiferromagnetic intermolecular interactions and/or zero field splitting of the resulting ground state, which is responsible for the decrease of $\chi_M T$ at low temperatures.

Taking into account the centrosymmetric face-sharing defective dicubane-like structure of complex **5**, the magnetic data have been analysed with the following three-*J* Hamiltonian:

$$H = -J_1(S_{Ni1}S_{Ni2} + S_{Ni1*}S_{Ni2*}) - J_2(S_{Ni1}S_{Ni2*} + S_{Ni1*}S_{Ni2}) - J_3(S_{Ni2}S_{Ni2*})$$

where J_1, J_2 and J_3 describe the exchange pathway through the μ-phenoxido/$\mu_{1,1,1}$-methoxido/*syn-syn* acetate, μ-phenoxido/$\mu_{1,1,1}$-methoxido and di-$\mu_{1,1,1}$-methoxido bridges, respectively (see inset of Figure 10). The external Ni1 atoms are too far (5.417 Å) to have significant magnetic interactions and therefore, the magnetic exchange between them has not been taking into account. In order to avoid overparametrization we have fitted the data above 30 K to eliminate the effect of the anisotropy and possible intermolecular interactions. The best fit parameters were: J_1 = +4.2 cm^{-1}, J_2 = -4.8 cm^{-1}, J_3 = +11.5 cm^{-1} and g = 2.23 with R = 1.3 x 10^{-5}. These parameters indicate the presence of moderate ferromagnetic exchange interactions between Ni1-Ni2, Ni1*-Ni2* and Ni2-Ni2* ions and antiferromagnetic interactions between Ni1-Ni2* and Ni1*-Ni2 ions, which are competing interactions.

The magnetization (M) measured at 2 K for compound **5** exhibits a gradual increase with the increasing field but does not reach saturation even at 10 T. The fact that the

magnetization continues increasing at higher fields could be due to the presence of significant anisotropy in the ground state and/or accessible low-lying excited states that are partially populated at 2 K.

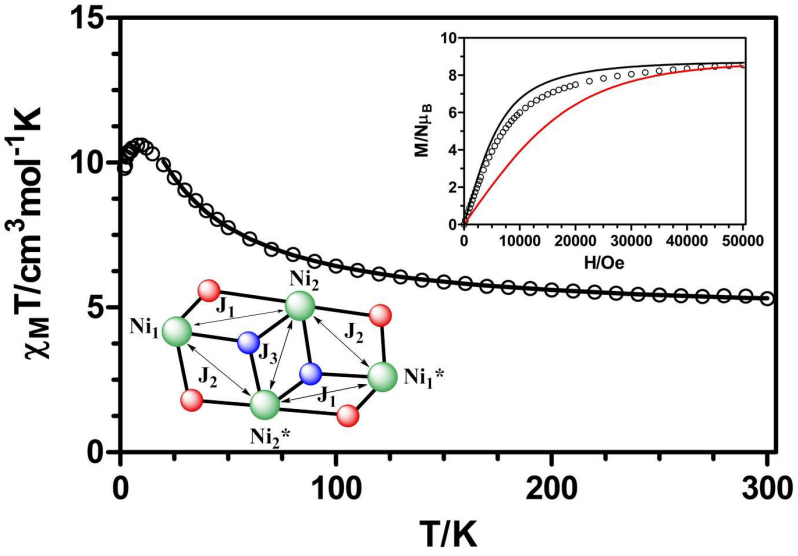

Figure 11. Temperature dependence of the $\chi_M T$ product for **6** in the 2-300 K range. The solid line is generated from the best fit to the magnetic parameters. Inset top: field dependence of the magnetization for **6**. The black and red solid lines represent the Brillouin function for an S = 4 ground state and for the sum of four Ni^{II} ions with S = 1, respectively. Inset bottom: magnetic exchange pathways in compound **6**.

Due to the similarity on the structure of complex **6** with **5**, we have used the same Hamiltonian as for **5**, where J_1, J_2 and J_3 account for μ-phenoxido/$\mu_{1,1,1}$-azido/*syn-syn* acetate, μ-phenoxido/$\mu_{1,1,1}$-azido and di-$\mu_{1,1,1}$-azido exchange pathways, respectively (see inset Figure 11). The fit of the experimental susceptibility data above 20 K, which are not affected by the effects of *D* and intermolecular interactions, lead to the following best fit parameters: J_1 = +5.6 cm^{-1}, J_2 = +9.8 cm^{-1}, J_3 = +43.8 cm^{-1} and g = 2.18 with R = 2.3x10^{-5}.

The field dependence of the molar magnetization at 2 K for compound **6** (Figure 11, inset) is slightly below the Brillouin function for a S = 4 and g = 2.18, which corroborates the existence of ferromagnetic interactions between the Ni^{2+} ions. The deviation from the Brillouin function is more likely due to the zero-field splitting effects of the S = 4 ground state and possible intermolecular interactions.

In order to know the nature and magnitude of the magnetic coupling interactions in complexes **3** and **4**, and to support the experimental *J* values found for complexes **2**, **5**

and **6** we carried out DFT calculations on the X-ray structures using the broken-symmetry approach. Table 1 presents the summary of the calculated *J* values of all the compounds.

The calculated magnetic exchange coupling constants for **3** and **4** are weak in agreement with the experimental results. Thus, for complex **3**, the calculated magnetic exchange coupling through the di-μ-phenoxido/μ-*syn-syn* acetate triple bridge is ferromagnetic in nature with J = +2.90 cm^{-1}. For **4** the magnetic exchange couplings through the double μ-phenoxido/μ-water bridges are antiferromagnetic with J_1 = -3.5 cm^{-1} and J_2 = -5.0 cm^{-1} for Ni1-Ni2 and Ni2-Ni3 ions, respectively, whereas the magnetic coupling between the external Ni^{2+} ions is, as expected, much weaker with J_3 = -0.85 cm^{-1} (see inset figure 9).

Table 1. Magnetic pathways and magnetic coupling constants for complexes **2**-**6**.

Compound	Magnetic pathways	J_{exp} (cm^{-1})	J_{calc} (cm^{-1})
2	Di-μ-phenoxido	-12.6	-16.0
3	Di-μ-phenoxido/*syn-syn* acetate	-	+2.90
4	μ-phenoxido/μ-water (Ni1-Ni2)	-	-3.5 (J_1)
	μ-phenoxido/μ-water (Ni2-Ni3)	-	-5.0 (J_2)
	External Ni^{2+} ions (Ni1-Ni3)	-	-0.85 (J_3)
5	μ-phenoxido/$\mu_{1,1,1}$-methoxido/*syn-syn* acetate	+4.2 (J_1)	+10.0 (J_1)
	μ-phenoxido/$\mu_{1,1,1}$-methoxido	-4.8 (J_2)	-7.4 (J_2)
	di-$\mu_{1,1,1}$-methoxido	+11.5 (J_3)	+11.2 (J_3)
	External Ni^{2+} ions (Ni1-Ni1*)	-	+0.06 (J_4)
6	μ-phenoxido/$\mu_{1,1,1}$-azido/*syn-syn* acetate	+5.6 (J_1)	+13.35 (J_1)[a]
	μ-phenoxido/$\mu_{1,1,1}$-azido	+9.8 (J_2)	+15.05 (J_2)[a]
	di-$\mu_{1,1,1}$-azido	+43.8 (J_3)	+34.65 (J_3)[a]
	External Ni^{2+} ions (Ni1-Ni1*/Ni3-Ni3*)	-	-0.11 (J_4)[a]

[a]These values are the media calculated for both independent Ni_4 units. Unit 1 (composed by Ni1 and Ni2): J_1 = +14.8 cm^{-1}, J_2 = +15.6 cm^{-1}, J_3 = +38.6 cm^{-1}, J_4 = -0.152 cm^{-1}; unit 2: (composed by Ni3 and Ni4): J_1 = +11.9 cm^{-1}, J_2 = +14.5 cm^{-1}, J_3 = +30.7 cm^{-1}, J_4 = -0.077 cm^{-1}.

For complexes **2**, **5** and **6** the calculated values are in rather good agreement in sign and magnitude with those of the experimental results. The difference between the experimental and calculated values could be due to limitations inherent to the method, and, as usual, the former are smaller than the latter ones.

The calculated spin density distributions for the ground state in complexes **2**-**6** (the spin density of **6** is given as a example in Figure 12, whereas those for the rest of complexes are given in Figure S5) show the predominance of the delocalization mechanism through a σ type exchange pathways involving the dx^2-y^2 and dz^2 magnetic orbitals of the nickel(II) atoms and the *p* orbitals of the ligand bridging donor groups (see Table S3). As expected, the spin density is mainly found at the nickel(II) ions, with values in the range 1.65-1.74 e).

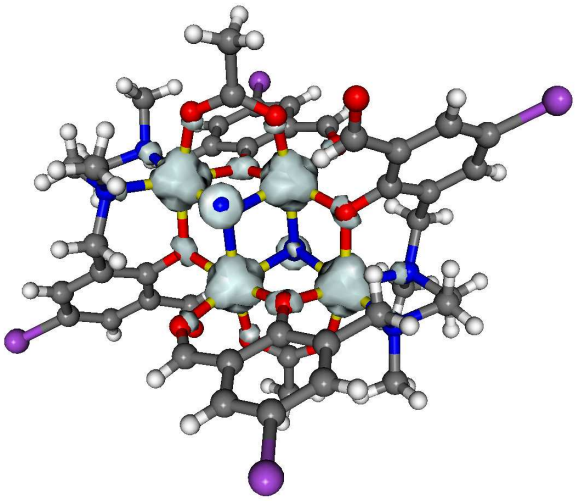

Figure 12. Calculated spin densities for the quintuplet state of **6**. The isodensity surfaces represented correspond to a cut-off value of 0.012 e bohr^{-3}. Grey and blue colors correspond to positive and negative values, respectively.

Finally, it is worth mentioning that dynamic alternating current (ac) magnetic susceptibility measurements as a function of temperature at different frequencies were performed on complex **6**, which exhibits a relatively large ground spin state S =4. The compound does not show frequency dependency of the in-phase (χ'_M) and out-of-phase signals (χ''_M) even in the presence of an external dc field of 1000G and, therefore, does not exhibit SMM behaviour above 2 K.

Magneto-structural correlations

Let us start with complex **2**. Experimental and theoretical magneto-structural correlations carried out by our group[7a] and others[7b-f] have clearly shown that the major factor controlling the exchange coupling in planar hydroxido-, alkoxido- and phenoxido-Ni(μ-O_2)Ni complexes is the bridging Ni-O-Ni angle (θ). According to these magneto-structural correlations, ferromagnetic coupling is expected below the critical Ni-O-Ni

angle of ~ 96-98° and the exchange coupling becomes antiferromagnetic above it. Moreover, it has also been seen from theoretical studies[7a] that the out-of-plane displacement of the phenyl carbon atom from the Ni_2O plane (τ) and the hinge angle between the O-Ni-O planes in the bridging fragment (β) also play a significant role in determining the magnitude of the magnetic coupling. Thus, the AF interaction increases when τ and/or β decrease so it is reasonable to think that small θ angles (close to 90-95°) combined with larger τ (>30-40°) and β (>20°) angles should lead to weak AF or even F interactions in this kind of compounds. Taking these magneto-structural correlations into account, the antiferromagnetic interaction between the Ni^{II} ions observed for **2** is not unexpected as the mean θ, τ and β angles are of 101.5°, 20.9° and 8.86°, respectively.

In the case of complex **3**, the mean θ, τ and β angles are 94.74°, 37.05° and 33.60°, respectively, and therefore a weak F interaction between the Ni^{II} ions is expected, which is in good agreement with the calculated value and experimental results. Moreover, the presence of an additional *syn-syn* acetate bridge between the two Ni (II) centres favours the ferromagnetic interaction due to the counter-complementarity effects between the di-μ-phenoxido and carboxylate bridging ligands.[26] In fact, DFT calculations on di-μ-phenoxido/μ-acetate compounds where the *syn-syn* acetate bridge has been substituted by two water molecules clearly show that this bridging group provides ferromagnetic contribution to the exchange through orbital countercomplementary.[7a]

The trinuclear Ni_3 complex **4** has two non-equivalent double μ-phenoxido/μ-water magnetic exchange pathways between the central and external Ni^{2+} ions, which are described by J_1 and J_2. It should be noted that, to the best of our knowledge, **4** is only the second example of a structurally and magnetically characterized Ni^{II} polynuclear complex where the mixed double μ-phenoxido/μ-water bridge is present.[27] The first example is the tetranuclear complex $[Ni_4L^2(\mu_3\text{-}OH)(\mu_2\text{-}H_2O)_2(ClO_4)](ClO_4)_2\cdot 2CH_3COCH_3\cdot H_2O$ (H_4L^2 = 36-membered octaaminotetraphenol macrocyclic ligand),[27] which exhibits an antiferromagnetic exchange coupling through this mixed double bridge with J = -8.1 cm^{-1}. However, this value is not comparable to that of **4** because, in order to avoid overparametrization, the four exchange pathways with Ni-O-Ni angles ranging from 78.8° to 132.3° were considered to be equivalent. For the Ni-O_{water}-Ni angles of 94.13° and 94.92° ferromagnetic couplings are expected whereas the Ni-$O_{phenoxido}$-Ni angles of 100.96° and 101.27° should transmit antiferromagnetic interactions. The calculated magnetic exchange coupling constants (J_1 = -3.5 cm^{-1} and J_2 = -5.0 cm^{-1}) indicate that antiferromagnetic interactions prevail over the ferromagnetic

ones in **4**. On the other hand, the weak antiferromagnetic coupling between the external Ni^{2+} ions (J_3 = -0.85 cm^{-1}) is in good agreement with the expected for two unbridged Ni^{2+} ions with a Ni···Ni distance of 5.047 Å.

To the best of our knowledge, complex **5** is the first example reported to date with this type of structure. The defective dicubane core of **5** exhibits three different types of exchange pathways between the Ni^{2+} ions: (i) triple μ-phenoxido/$\mu_{1,1,1}$-methoxido/*syn-syn* acetate bridges (described by J_1), (ii) double μ-phenoxido/$\mu_{1,1,1}$-methoxido bridges (described by J_2) and (iii) double di-$\mu_{1,1,1}$-methoxido bridge (described by J_3). Let us start with the first exchange pathway. As in complex **3**, the weak ferromagnetic interaction between the Ni^{II} ions found for the magnetic exchange pathway (i) is not unexpected in view of the values for the angles in the phenoxido/$\mu_{1,1,1}$-methoxido Ni-(O_2)-Ni bridging fragment (θ = 94.2°, τ = 34.25° and β = 19.11°) and the counter-complementarity effects *syn-syn* acetate bridges. As far as we know, the magnetic exchange pathway through the double μ-phenoxido/$\mu_{1,1,1}$-methoxido mixed bridge (ii), has been observed for the first time in Ni^{II} containing complexes. The antiferromagnetic nature of the experimental magnetic coupling constant through this pathway is not unexpected taking into account the mean values of the θ, τ and β angles with values of 101.7°, 41.8° and 6.12°, respectively. Regarding the magnetic exchange pathway through the di-$\mu_{1,1,1}$-methoxido bridge (iii), the values of the θ and τ angles in the Ni(O_2)Ni symmetric planar bridging fragment (97.1° and 52.7°, respectively) predict weak F interactions, which again matches well with the experimental and theoretical results. The magnitude of the ferromagnetic interaction through pathways (i) and (iii) are in accordance with the exchange interactions found in the four structurally similar complexes with the general formula $[Ni_4(L^3)_2(\mu\text{-}N_3)_2(\mu\text{-}OAc)_2(\mu\text{-}OMe)_2]\cdot xCH_3OH\cdot yH_2O$ (HL^3 = 2,6-bis[(2-hydroxy-ethylimino)-methyl]-4-methylphenol and derivatives), which range from +4.32 to +11.6 cm^{-1}.[9b,28]

Finally, as far as we know, complex **6** is also the first example reported to date with this type of structure. This complex exhibits the same structure as **5**, but in which the $\mu_{1,1,1}$-methoxido bridges are replaced by $\mu_{1,1,1}$-azido bridges. Therefore, **6** exhibits three different types of exchange pathways between the Ni^{2+} ions: (i) triple μ-phenoxido/$\mu_{1,1,1}$-azido/*syn-syn* acetate bridges (described by J_1), (ii) double μ-phenoxido/$\mu_{1,1,1}$-azido bridges (described by J_2) and (iii) double di-$\mu_{1,1,1}$-azido bridge (described by J_3). It is well known that azido bridges generally transmit ferromagnetic interactions between the Ni^{2+} ions and, therefore, the change of methoxido by azido bridges is expected to lead to

stronger ferromagnetic interactions, which is in accordance with the experimental and theoretical results.

It should be noted that **6** is only the third nickel complex containing a mixed triple μ-phenoxido/μ-azido/*syn-syn* acetate bridge (i).[10,29] The first example is the trinuclear bent complex $[Ni_3L^3{}_2(OAc)_2(\mu_{1,1}\text{-}N_3)_2(H_2O)_2]$ (L^3 = 2-[(3-dimethylaminopropylimino)-methyl]-phenol)[29] that exhibits a ferromagnetic exchange coupling through this mixed triple bridge with J =+16.51 cm^{-1}. The second example is the zig-zag hexanuclear complex $[Na_2Ni_4(\mu\text{-}L^1)_2(\mu\text{-}OAc)_2(\mu\text{-}N_3)_4(CH_3OH)_4]\cdot 2CH_3OH$ (H_2L^1 is *N*,*N*'-dimethyl-*N*,*N*'-bis(2-hydroxy-3-methoxy-5-methylbenzyl)ethylenediamine) with J_1 = +28.8 cm^{-1}.[10] The observed ferromagnetic interactions in these complexes through the exchange pathway (i) are not only due to the presence of $\mu_{1,1,1}$-azido bridges and relatively small Ni-$O_{phenoxido}$-Ni angles but also to countercomplementarity effect of the *syn-syn* acetate bridge. Therefore, the ferromagnetic exchange coupling observed for **4** via the exchange pathaway (i) with Ni-$O_{phenoxido}$-Ni and Ni-O_{azide}-Ni mean angles of 96.2° and 90.73° is not unexpected.

Regarding the exchange pathway (ii), as far as we know, only another example of a complex containing a double phenoxido/$\mu_{1,1,1}$-azide mixed bridge between Ni^{II} ions has been reported so far.[10] In this complex, $[Ni_4(\mu\text{-}L^1)_2(\mu\text{-}N_3)_4(CH_3OH)_2]\cdot 2CH_3OH$ (H_2L^1 is *N*,*N*'-dimethyl-*N*,*N*'-bis(2-hydroxy-3-methoxy-5-methylbenzyl)ethylenediamine), the exchange pathway (ii) transmits a ferromagnetic interaction with J = +2.0 cm^{-1}. It should be noted that recent DFT theoretical studies[8] on Ni^{II} model complexes containing double μ-phenoxido/$\mu_{1,1}$-azido bridges have predicted that the ferromagnetic interaction increases with increasing the Ni-N_{azide}-N/Ni-N_{azide} ratio and the asymmetry of the two Ni-N_{azide} distances, and decreases with increasing the Ni-$O_{phenoxido}$-Ni/Ni-$O_{phenoxido}$ ratio, so that phenoxido and $\mu_{1,1}$-azide bridges have countercomplementary effects on the magnetic exchange coupling. Assuming that these magneto-structural correlations are also valid for Ni^{II} complexes with double μ-phenoxido/$\mu_{1,1,1}$-azido bridges, for complex **3**, with a similar Ni-N_{azide}-N/Ni-N_{azide} ratio to that observed in $[Ni_4(\mu\text{-}L^1)_2(\mu\text{-}N_3)_4(CH_3OH)_2]\cdot 2CH_3OH$ but with a smaller Ni-$O_{phenoxido}$-Ni/Ni-$O_{phenoxido}$ ratio, a larger ferromagnetic interaction is expected through this exchange pathway, which agrees well with the experimental and theoretical results.

Finally, as for the exchange pathway (iii) with a double ($\mu_{1,1,1}$-N_3)-bridging unit, the ferromagnetic nature of the experimental magnetic coupling constant is not unexpected as

it is well known that $\mu_{1,1,1}$-N_3 bridges transmit ferromagnetic interactions, which increase with the increase of the Ni-N_{azide}-Ni angle and decrease with the deviation of the $\mu_{1,1,1}$-azide bridging ligand from the Ni-$(N_{azide})_2$-Ni plane.[10] Taking into account these magneto-structural correlations, the low value found for this exchange pathway in **6** (J_3 =+43.8 cm^{-1}) compared to those observed for planar ($\mu_{1,1}$-N_3)-bridged dinuclear Ni^{II} complexes (typically between +60 and +80 cm^{-1}),[10,30] could be due to the low Ni-N_{azide}-Ni angle of 97.35° and the large deviation of the $\mu_{1,1,1}$-azide bridging ligand from the Ni-(N_{azide})-Ni plane of 52.9°.

Conclusions

Using the flexible polytopic ligand N,N'-dimethyl-N,N'-bis(2-hidroxy-3-formyl-5-bromo-benzyl)ethylenediamine and different anionic coligands and reaction conditions (metal to ligand molar ratio and solvent) we were able to prepare six Ni^{II} complexes, ranging from mononuclear to tetranuclear compounds, with structural and magnetic diversity, in which the ligand adopts a variety of bridging coordination modes. Thus, the dinuclear complexes exhibit either double di-μ-phenoxido or triple di-μ-phenoxido/μ-*syn syn* acetate bridges, which transmit medium AF and very weak F interactions, respectively. The Ni_3 complex presents a bent structure with rare double μ-phenoxido-μ-water bridges between central and external Ni^{II} ions, which transmit very weak AF interactions. The weak magnetic exchange interactions for the Ni3 complex and the Ni2 complex with triple di-μ-phenoxido/μ-*syn syn* acetate bridges were determined by DFT calculations on their respective X-ray crystal structures. Their sign and magnitude are related to the values of the Ni-O-Ni bridging angles and, in the case of the latter, to the additional countercomplementarity effect exerted by the μ-*syn syn* acetate bridging group. Two Ni4 complexes were obtained, which present similar defective dicubane like topologies with three distinct types of bridges between the Ni^{II} ions. The main structural difference between both Ni4 complexes is the presence in one of them of $\mu_{1,1,1}$-methoxido bridges and in the other one of $\mu_{1,1,1}$-azido bridges. In the Ni_4 compound containing methoxido group, the triple mixed μ-phenoxido/$\mu_{1,1,1}$-methoxido/*syn-syn* acetate bridge and the double di-μ-phenoxido bridge propagate weak F interactions between the Ni^{II} ions, whereas the unusual μ-phenoxido/$\mu_{1,1,1}$-methoxido bridge mediates weak AF interactions. It should be noted that the change of $\mu_{1,1,1}$-methoxido bridges by $\mu_{1,1,1}$-azido bridges provokes that all the magnetic pathways transmit ferromagnetic interactions,

which are stronger that those found for the compound containing $\mu_{1,1,1}$-methoxido bridges. The sign and nature of the experimental *J* values found for these Ni4 species were supported by DFT calculations.

Electronic Supplementary information (ESI)

X-ray crystallographic data for **1-6**, including data collection, refinement and selected bond lengths and angles. Figures and tables of the spin density distribution for compounds **2-6**.

Acknowledgements

Financial support from Ministerio de Economía y Competitividad (MINECO) for Project CTQ-2011-24478, the Junta de Andalucía (FQM-195 and the Project of excellence P11-FQM-7756), the University of Granada and Universidad del País Vasco are grateful acknowleged. We would like to thank the Centro de Supercomputación de la Universidad de Granada for computational resources. I. O. is grateful to the Departamento de Educación, Universidades e Investigación del Gobierno Vasco for a predoctoral fellowship. Technical and human support provided by SGIker (UPV/EHU, MINECO, GV/EJ, ERDF and ESF) is gratefully acknowledged.

Notes and References

[1] (*a*) *Concepts and Models in Bioinorganic Chemistry*, H. B. Kraatz and N. Metzler-Nolte (Ed), Wiley-VCH, Weinheim, Germany, 2006; (*b*) I. Bertini, H. B. Gray, E. I. Stiefeld, and J. S. Valentine, *Biological Inorganic Chemistry: Structure and Reactivity*, University Science Books, 2007; (*c*) *Handbook of Metalloproteins*, A. Messerschmidt, R. Huber, T. Poulos and K. Wieghardt (Eds.), Wiley, Chichester, 2001; (*d*) *Nickel and its surprising impact in nature. Metal Ions in Life Sciences*, *vol. 2*; A. Sigel, H. Sigel and R. K. Sigel (Eds.), John Wiley and Sons, Chichester, 2007; (*e*) J. L. Boer, S. B. Mulrooney and R. P.

Hausinger, *Arch. Biochem. Bipophys.* 2014, **544C**, 142 - 152 and references therein; (*f*) S. W. Ragsdale, *J. Biol. Chem.,* 2009, **284**, 18571–18575.

[2] *Magnetism: Molecules to Materials, vols. I–V,* J. S. Miller and M. Drillon, (Ed.)*,* Wiley-VCH*,* Weinheim, Germany, 2001-2004.

[3] (*a*) D. Gatteschi, R. Sessoli R. and J. Villain, *Molecular Nanomagnets*, Oxford University Press, Oxford, UK, 2006; (*b*) G. Aromí and E. K. Brechin, *Struct. Bond*., 2006, **122**, 1–67; (*c*) *Molecular Cluster Magnets.* R. E. P. Winpenny (Ed.), World Scientific Books, Singapore, 2011.

[4] J. N. Rebilly and T. Mallah; *Struct. Bond*., 2006, **122**, 103–131.

[5] (*a*) A. R. Rocha, V. M. García-Suárez, S. W. Bailey, C. J. Lambert, J. Ferrerand and S. Sanvito, *Nat. Mater.,* 2005, **4***,* 335-339; (*b*) L. Bogani and W. Wernsdorfer, *Nat. Mater*., 2008, **7***,* 179-186; (*c*) M. Affronte, *Mater. Chem*., 2009, **19***,* 1731-1737; (*d*) M. N. Leuenberger and D. Loss, *Nature*, 2001, **410***,* 789-793; (*e*) A. Ardavan, O. Rival, J. J. L. Morton, S. J. Blundell, A. M. Tyryshkin, G. A. Timco, G. A. and R. E. P. Winpenny, *Phys. Rev. Lett.*, 2007, **98***,* 057201-057204; (*f*) P. C. E. Stamp and A. Gaita-Ariño, *J. Mater. Chem*., 2009, **19***,* 1718-1730.

[6] (*a*) A. K. Boudalis, M. Pissas, C. P. Raptopoulou, V. Psycharis, B. Abarca and R. Ballesteros, *Inorg. Chem*, 2008, **47**, 10674-10681; (*b*) A. Ferguson, J. Lawrence, A. Parkin, J. Sanchez-Benitez, K. V. Kamenev, E. K. Brechin, W. Wernsdorfer, S. Hill, and M. Murrie, *Dalton Trans.,* 2008, 6409-6414; (*c*) A. Bell, G. Aromí, S. J. Teat, W. Wernsdorfer, and R. E. P. Winpenny, *Chem. Commun.*, 2005, 2808-2810; (*d*) D. I. Alexandropoulos, C. Papatriantafyllopoulou, G. Aromi, O. Roubeau, S. J. Teat, S. P. Perlepes, G. Christou amd T. C. Stamatatos, *Inorg. Chem.,* 2010, **49**, 3962-3964; (*e*) S. Petit, P. Neugebauer, G. Pilet, G. Chastanet, A. L. Barra, A. B. Antunes, W. Wernsdorfer, and D. Luneau, *Inorg. Chem.,* 2012, **51**, 6645-6654 and references therein; (*f*) R. Biswas, Y. Ida, M. L. Baker, S. Biswas, P. Kar, H. Nojiri, T. Ishida, and A. Ghosh, *Chem. Eur. J*., 2013, **19**, 3943-3953; (*g*) H. Andres, R. Basler, A. J. Blake, C. Cadiou, G. Chaboussant, C. M. Grant, H. U. Güdel, M. Murrie, S. Parsons, C. Paulsen, F. Semadini, V. Villar, W. Wernsdorfer and R. E. P. Winpenny, *Chemistry,* 2002, **8**, 4867–4876; (*h*) R. T. W. Scott, L. F. Jones, I. Tidmarsh; S. B. Breeze, R. H. Laye, J. Wolowska, D. J. Stone, A. Collins, S. Parsons, W. Wernsdorfer, G. Aromi, E. J. L. McInnes and E. K. Brechin, *Chem. Eur. J*., 2009, **15**, 12389-12398; (i) S. Hameury, L. Kayser, R. Pattacini, G. Rogez, W. Wernsdorfer and P. Braunstein, *Dalton Trans*., 2013, **42**, 5013-5024.

[7] (*a*) M. P. Palacios, A. J. Mota, J. E. Perea-Buceta, F. J. White, E. K. Brechin and E. Colacio, *Inorg. Chem.*, 2010, **49**, 10156-10165; (*b*) R. Biswas, S. Giri, S. K. Saha and A. Ghosh, *Eur. J. Inorg. Chem.*, 2012, 2916–1927; (*c*) K. K. Nanda, L. K. Thompson, J. N. Bridson and K. Nag, *J. Chem. Soc. Chem. Commun*., 1994, 1337-1338; (*d*) M. A. Halcrow, J. S. Sun, J. C. Huffman and G. Christou, *Inorg. Chem.*, 1995, **34**, 4167-4177; (*e*) J. M. Clemente-Juan, B. Chansou, B. Donnadieu and J. P. Tuchages, *Inorg. Chem.*, 2000, **39**, 5515-5519; (*f*) X. H. Bu, M. Du, L. Zhang, D. Z. Liao, J. K. Tang, R. H. Zhang and M. Shionoya, *J. Chem. Soc., Dalton Trans.*, 2001, 593-598.

[8] S. Sasmal, S. Hazra, P. Kundu, S. Dutta, G. Rajaraman, E. C. Sañudo and S. Mohanta, *Inorg. Chem.,* 2011, **50**, 7257-7267.

[9] (*a*) P. Mukherjee, M. G. B. Drew, C. J. Gómez-García and A. Gosh, *Inorg. Chem*., 2009, **48**, 5848-5860; (*b*) S. S. Tandon, S. D. Bunge, R. Rakosi, Z. Xu and L. K. Thompson, *Dalton Trans*., 2009, 6536-6551. (*c*) A. Biswas, L. K. Das, M. G. Drew, G. Aromí, P. Gámez and A. Gosh, *Inorg. Chem*., 2012, **51**, 7993-8001; (*d*) A. K. Gosh, M. Shatruk, V. Bertolasi, K. Pramanik and D. Ray, *Inorg. Chem.,* 2013, **52**, 13894-13903.

[10] L. Botana, J. Ruiz, A. J. Mota, A. Rodríguez-Diéguez, J. M. Seco, I. Oyarzabal and E. Colacio, *Dalton Trans*., 2014, **43**, 13509-13524.

[11] M. Yonemura, Y. Matsumura, M. Ohba, H. Okawa and D. E. Fenton, *Chem. Lett*. 1996, 601-602.

[12] (*a*) A. D. Becke, *Phys. Rev. A*, 1988, **38**, 3098–3100; (*b*) C. T. Lee, W. T. Yang and R. G. Parr, *Phys. Rev. B: Condens. Matter*, 1988, **37**, 785–789; (*c*) A. D. Becke, *J. Chem. Phys*., 1993, **98**, 5648–5652.

[13] M. J. Frisch, G. W. Trucks, H. B. Schlegel, G. E. Scuseria, M. A. Robb, J. R. Cheeseman, J. A. Montgomery Jr., T. Vreven, K. N. Kudin, J. C. Burant, J. M. Millam, S. S. Iyengar, J. Tomasi, V. Barone, B. Mennucci, M. Cossi, G. Scalmani, N. Rega, G. A. Petersson, H. Nakatsuji, M. Hada, M. Ehara, K. Toyota, R. Fukuda, J. Hasegawa, M. Ishida, T. Nakajima, Y. Honda, O. Kitao, H. Nakai, M. Klene, X. Li, J. E. Knox, H. P. Hratchian, J. B. Cross, C. Adamo, J. Jaramillo, R. Gomperts, R. E. Stratmann, O. Yazyev, A. J. Austin, R. Cammi, C. Pomelli, J. W. Ochterski, P. Y. Ayala, K. Morokuma, G. A. Voth, P. Salvador, J. J. Dannenberg, V. G. Zakrzewski, S. Dapprich, A. D. Daniels, M. C. Strain, O. Farkas, D. K. Malick, A. D. Rabuck, R. Raghavachari, J. B. Foresman, J. V. Ortiz, Q. Cui, A. G. Baboul, S. Clifford, J. Cioslowski, B. B. Stefanov, G. Liu, A. Liashenko, P. Piskorz, I. Komaromi, R. L. Martin, D. J. Fox, T. Keith, M. A. Al-Laham,

C. Y. Peng, A. Nanayakkara, M. Challacombe, P. M. W. Gill, B. Johnson, W. Chen, M. W. Wong, C. Gonzalez and J. A. Pople, *GAUSSIAN 03* (*Revision C.0*), Gaussian, Inc., Wallingford, CT, 2004.

[14] G. B. Bacskay, *Chem. Phys*., 1981, **61**, 385–404.

[15] A. Schäfer, C. Huber and R. Ahlrichs, *J. Chem. Phys*., 1994, **100**, 5829–5835.

[16] *Jaguar 7.6*, Schrödinger, Inc., Portland, OR, 2009.

[17] (*a*) E. Ruiz, J. Cano, S. Alvarez and P. Alemany, *J. Comput. Chem*., 1999, **20**, 1391–1400; (*b*) E. Ruiz, S. Alvarez, A. Rodríguez-Fortea, P. Alemany, Y. Puoillon and C. Massobrio, in *Magnetism: Molecules to Materials*, ed. J. S. Miller and M. Drillon, Wiley-VCH, Weinheim, 2001, vol. II, p. 5572; (*c*) E. Ruiz, A. Rodríguez-Fortea, J. Cano, S. Alvarez and P. Alemany, *J. Comput. Chem*., 2003, **24**, 982–989; (*d*) E. Ruiz, S. Alvarez, J. Cano and V. Polo, *J. Chem. Phys*., 2005, **123**, 164110/1-164110/7.

[18] *CrysAlisPro Software System*, Agilent Technologies UK Ltd, Oxford, UK, 2012.

[19] G. M. Sheldrick, *Acta Crystallogr., Sect. A: Fundam. Crystallogr*., 2008, **64**, 112-122.

[20] A. L. Spek, *PLATON-4*, *A Multipurpose Crystallographic Tool*, University of Utrecht, The Netherlands, 1994.

[21] I. Oyarzabal, J. Ruiz, J. M. Seco, M. Evangelisti, A. Camón, E. Ruiz, D. Aravena and E. Colacio, *Chem. Eur. J*. **2014,** *20*, 14262-14269.

[22] (*a*) J. Ruiz, A. J. Mota, A. Rodríguez-Diéguez, S. Titos, J. M. Herrera, E. Ruiz, E. Cremades, J. P. Costes and E. Colacio, *Chem. Commum*. 2012, **48**, 7916-7918 ; (*b*) J. P. Costes, F. Dahan and F. Nicodème, *Inorg. Chem.,* 2003, **42**, 6556-6563.

[23] R. Biswas, P. Kar, Y. Song and A. Ghosh, *Dalton Trans*. 2011, 40, 5324-5331.

[24] A. J. Mota, A. Rodríguez-Diéguez, M. A. Palacios, J. M. Herrera, D. Luneau and E. Colacio, *Inorg. Chem.,* 2010, **49**, 8986-8996.

[25] N. F. Chilton, R. P. Anderson, L. D. Turner, A. Soncini and K. S. Murray, *J. Comput. Chem*., 2013, **34**, 1164–1175.

[26] (*a*) P. Mukherjee, M. G. B. Drew, V. Tangoulis, M. Estrader, C. Diaz and A. Ghosh, *Inorg. Chem. Commun*., 2009, **12**, 929-932; (*b*) J. Ruiz, A. J. Mota, A. Rodríguez-Diéguez, I. Oyarzabal, J. M. Seco and E. Colacio, *Dalton Trans*., 2012, **41**, 14265-14273.

[27] (a) S. Mohanta, K. K. Nanda, R. Werner, W. Haase, A. K. Mukherjee, S. K. Dutta and K. Nag, Inorg. Chem., 1997, **36**, 4656-4664; (b) K. K. Nanda, K. Venkatsubramanian, D. Majumdar and K. Nag, *Inorg. Chem*., 1994, **33**, 1581-1582.

[28] S.-Y. Lin, G.-F. Xu, L. Zhao, Y.-N. Guo, J. Tang and Q.-L. Wang, *Inorg. Chim. Acta*, 2011, 173-178.

[29] R. Biswas, S. Mukherjee, P. Kar and A. Gosh, *Inorg Chem*., 2012, **51**, 8150-8160.

[30] (*a*) A. Escuer, J. Esteban, S. P. Perlepes, T. C. Stamatatos, *Coord.Chem. Rev*., 2014, **275**, 87-129; (b) A. Solanki, M. Monfort and S. B. Baran Kumar, *J. Mol. Struct*. 2013**,** **1050**, 197–203.

Experimental and theoretical magneto-structural correlations and DFT calculations carried out in six novel NiII complexes with uncommon **structures**